Journal of Environmental Radioactivity 225 (2020) 106420

Contents lists available at ScienceDirect

Journal of Environmental Radioactivity

journal homepage: http://www.elsevier.com/locate/jenvrad

A full-scale experimental study of sub-slab pressure fields induced by underground perforated pipes as a soil depressurisation technique in radon mitigation

Borja Frutos [a,*], Isabel Sicilia [a], Oscar Campo [a], Sofía Aparicio [b], Margarita González [b], José Javier Anaya [b], Daniel Rábago [c], Carlos Sainz [c]

[a] Eduardo Torroja Institute for Construction Science, IETcc (National Research Council, CSIC), Madrid, Spain
[b] Leonardo Torres Quevedo Institute for Physical and Information Technologies (ITEFI, National Research Council, CSIC), Madrid, Spain
[c] Radon Group, University of Cantabria, Santander, Spain

ARTICLE INFO

Keywords:
Radon mitigation
Soil depressurisation system
Perforated pipe system
Gravel bed
Full-scale concrete slab
Multi-sensor monitoring system

ABSTRACT

Sub-slab depressurisation systems have proven to effectively mitigate radon entry. A poor understanding of the fluid physics underlying the technique has been shown to lower the success rate substantially. This article describes a study of pressure fields in a sub-slab gravel bed induced by a soil depressurisation system consisting of perforated pipes run under the slab at a depth of 75 cm. The advantage of the approach is that pipes can be laid from outside the building to be protected. The study was conducted on a large-scale experimental facility where the variations in morphology and scope of pressure fields with different pipe combinations could be monitored and characterised. The findings showed that pressure was uniform across the entire area in the gravel bed, whereas the sensors buried in natural soil showed pressure to depend on distance from the source. Pressure transfer to the sub-slab plane was also observed to vary depending on the active pipe. Air-flow resistance studies in the layers of soil lying between the pipes and the gravel delivered different results for each pipe. That finding would appear to be related to the presence of preferential pathways in some parts of the soil. Total pressure when several pipes were activated was observed to be practically the same as the sum of the pressures transferred by each when working separately. The correlation between extraction fan power and pressure generated was also analysed. These and other factors are discussed and analysed from a perspective of the understanding of such highly effective techniques.

1. Introduction

The identification of radon gas (Rn-222) as the second most frequent cause of lung cancer after smoking (IARC, 1998; WHO, 2009) has inspired many studies on its occurrence in residential environments (Gaskin et al., 2018; Ruano-Ravina et al., 2003). Radon is the natural decay product of radium-226, an element widespread in the Earth's crust (Nazaroff et al., 1988). Exhalation from the soil is determined by substrate permeability, which governs advective gas mobility through the pores, along with its radium content and diffusivity (Friedmann et al., 2017; Neznal and Neznal, 2005). As a gas, radon is highly mobile and can penetrate buildings across fissures or cracks or permeable materials in contact with the soil. Earlier studies have explored the mechanics of gas movement from the soil to indoor areas based on convection and diffusion physics applied to materials, geometries and areas (Collignan et al., 2012; Font and Baixeras, 2003; Garbesi et al., 1999; Hintenlang, 1992; Vasilyev and Zhukovsky, 2013).

One of the most widespread and successful protection techniques (Roserens et al., 2000) used to reduce the flow of radon into buildings is soil depressurisation (SD) (Abdelouhab et al., 2010; Cosma et al., 2015; Frutos Vazquez et al., 2011; Fuente et al., 2019b; Scivyer, 2013). Effective depressurisation with the technique calls for an in-depth understanding of the parameters involved in gas mobility in soil (Jiránek et al., 2008).

SD is deployed to depressurise the soil under the entire area of a building slab (Health Canada, 2010), thereby inverting the pressure

* Corresponding author. Eduardo Torroja Institute for Construction Science, IETcc-CSIC, C/ Serrano Galvache 4, Madrid, 28033, Spain.
E-mail addresses: borjafv@ietcc.csic.es (B. Frutos), i.sicilia@csic.es (I. Sicilia), ocampovega@outlook.com (O. Campo), sofia.aparicio@csic.es (S. Aparicio), m.g.hernandez@csic.es (M. González), jj.anaya@csic.es (J.J. Anaya), rabagod@unican.es (D. Rábago), carlos.sainz@unican.es (C. Sainz).

https://doi.org/10.1016/j.jenvrad.2020.106420
Received 14 July 2020; Received in revised form 4 September 2020; Accepted 5 September 2020
Available online 17 September 2020

gradient between soil and building and consequently lowering advective radon flow. System efficacy for a given area depends on the area covered by the pressure field and its intensity. Both are clearly related to substrate air-flow resistance. Substrate permeability or the presence of sub-slab obstacles such as foundation lines are factors to be borne in mind in efficacy studies. Some of the effects of those characteristics have been studied with simulated models (Bonnefous et al., 1992; Diallo et al., 2015; Gadgil et al., 1991; Muñoz et al., 2017; Reddy et al., 1991). Entry rates across construction joints or accidental cracks in the slab have likewise been analysed (Andersen, 2001; Nazaroff, 1988).

The presence of negative pressure fields is favoured by more permeable sub-slab fill material such as gravel and hindered by compact natural soil (Diallo et al., 2018; Fuente et al., 2019a; Gadgil et al., 1991; Hung et al., 2019, 2018a). Pressure field constraint has also been observed when a slab fails to ensure impermeability between the soil and the indoor space (EPA Environmental Protection Agency, 1994; Frutos and Muñoz, 2018). Leaks through joints or cracks may connect the soil and indoor space, lowering the power of the air extraction system.

An understanding of those matters helps optimise depressurisation system design. Some have been studied experimentally by analysing the pressure fields associated with different slab/soil conditions (Collignan et al., 2004; Reddy et al., 1991; Robinson, 1996) and activating the system with sumps. In contrast, here the facility used consisted of perforated pipes (of the sort normally used for drainage). The aim was to furnish supplementary information as an aid to the design of such systems, for the experimental results differ when suction is applied through linear elements such as perforated pipes rather than discrete components such as sumps. The advantage to the former is that the pipes can be run underneath the foundations from outside the building.

The aim here was to further the understanding of pressure field behaviour in an SD system using different pipe setups. The pressure fields were characterised and data on their behaviour gathered with variations in fan power, pressure line arrangement and spacing under the slab, the number of lines deployed and the substrate type (gravel or natural soil). The study was conducted on a large-scale experimental slab, comparable to the size of the ground floor of a single family home and pressure was monitored with a double-decker sensor array.

The study of the radius of action of linear SD techniques and the variation in their pressure maps with changes in the aforementioned variables may help understand the mechanisms involved and hence optimise system design.

2. Materials and methods

The aim pursued was to characterise SD-induced pressure fields in the gravel and soil substrates under different linear suction conditions in a slab resting on gravel. The slab-on-gravel arrangement was chosen because it is routinely used in construction in many countries. The design flow and pressure in the depressurisation system were the only parameters analysed (Fowler et al., 1991).

The test facility, a concrete slab resting on gravel built on property belonging to the CSIC at Arganda del Rey, a town outside Madrid, was fitted with a continuous pressure monitoring system consisting in a double-decked grid of sensors positioned at two depths underneath the slab. The sensors recorded the difference between the outdoor pressure and the monitoring site value. A system of perforated pipes run into the soil parallel to the slab transferred the negative pressures generated by a mechanical extractor fan. A program using MATLAB environment (MathWorks, Natick, Massachusetts) was developed to interpret and display the pressure signals both on timelines and spatially on the slab. Substrate permeability was likewise characterised.

2.1. Concrete slab and sub-slab description

A 64 m^2 (8 × 8 m^2), 15 cm thick reinforced concrete slab was laid on a 20 cm thick bed of (20 mm–40 mm) gravel. This assembly is described in the Spanish technical building code (Ministerio de Fomento, 2006), chapter DB-HS1, for non-structural slabs. The natural soil over which the gravel was laid was neither compacted nor loosened. The gravel fill was deemed to have undergone no compaction other than as induced by the weight of the concrete slab, given the nature and grain size of the stone material. The 40 cm deep by 20 cm thick perimetric foundations impeded gravel contact with elements outside the slab. A flexible plastic membrane was placed over the gravel prior to pouring the concrete to prevent collapse. Slab construction is depicted in Fig. 1.

Upon conclusion, the slab joints and fissures were sealed with a polyurethane sealant, fibre mesh and elastomeric paint to prevent connections between the substrate and the outdoor air. The initial post-seal tests revealed that pressures had risen on the order of two-to three-fold, confirming that such slab flaws, which are common in this type of construction, may lower depressurisation system efficacy.

The geology of the soil on which the slab was built, determined on excavated samples, was observed to consist of three layers.

Layer 1 (0–0.4 m): silty loam with some jagged edge carbonated sand, rocks and considerable peat.
Layer 2 (0.4–1.1 m): gravel and rounded rock with silty carbonated matrix.
Layer 3 (1.1–1.5 m): sandy-clayey carbonated silt with some scattered rounded gravel.

The plane 2 sensors and perforated pipes were located in layers 1 and 2; the facility did not reach into layer 3.

Soil permeability was determined in situ with the instruments developed by RADON v. o.s (http://www.radon.eu). based on (KAŠPAR et al., 1993; Neznal and Neznal, 2005). The Radon-JOK permeameter pumps air out of the soil under constant negative pressure through a specially designed probe that interfaces with the soil across a constant and known 'shape factor'. The probe is driven into the ground behind a sharp sacrificial tip at the forward end, generating a constant air gap. Permeability at a given depth is calculated from a formula based on Darcy's law that relates the known air flow through the probe to pumping time. With a shape factor of 0.149 m, the Radon-JOK system

Fig. 1. a) Slab construction: foundations and gravel fill; b) finished slab.

delivers permeability readings across a range of 10^{-11} m^2 to 10^{-14} m^2.

A total of 10 permeability measurements were carried out: 5 at a depth of about 20 cm (gravel) and 5 at a depth of 60 cm (soil), made in the center and four corners of the slab. As expected, the values were distributed more uniformly in the gravel than in the soil. As the permeability levels recorded in the gravel were higher than the upper limit of the Radon-JOK range, however, additional laboratory tests were conducted to standard ASTM D6539 (ASTM International, 2013; Fuente et al., 2019a). The mean values found were:

Gravel: K $(9.0 \pm 3.5) \times 10^{-8}$ m^2

Soil: K $= (4 \pm 2) \times 10^{-12}$ m^2

Which lay within the range usually reported for the type of substrates at issue (Neznal et al., 2004).

2.2. Soil depressurisation system

The depressurisation system consisted of four 8 m long parallel perforated pipes spaced at 2 m on a horizontal plane 75 cm under the top of the slab. One (pipe AB), extended beyond the end of the slab, served as a control and was used to study the longitudinal pressure drop between the head and tail ends of the pipe. The findings are discussed in section 3.2.

The pipes were attached on the surface to an above-ground header pipe in turn connected to a mechanical fan that drove the system. Each perforated pipe had a cut-off valve to study the pressure fields when just one or any combination was activated.

The components of the test facility and nomenclature of the plane 1 measuring points are depicted in Fig. 2. Plane 2 were labelled as in plane 1 followed by 'prime' (').

The nomenclature was defined by the intersection between lines 1 to 5 and lines A to E, whilst the perforated pipes were labelled with the letters of the two flanking longitudinal lines (AB; BC; CD; DE).

Pipe AB was not included in the experimental findings discussed in section 3 due to deviations occurring when placed in the ground.

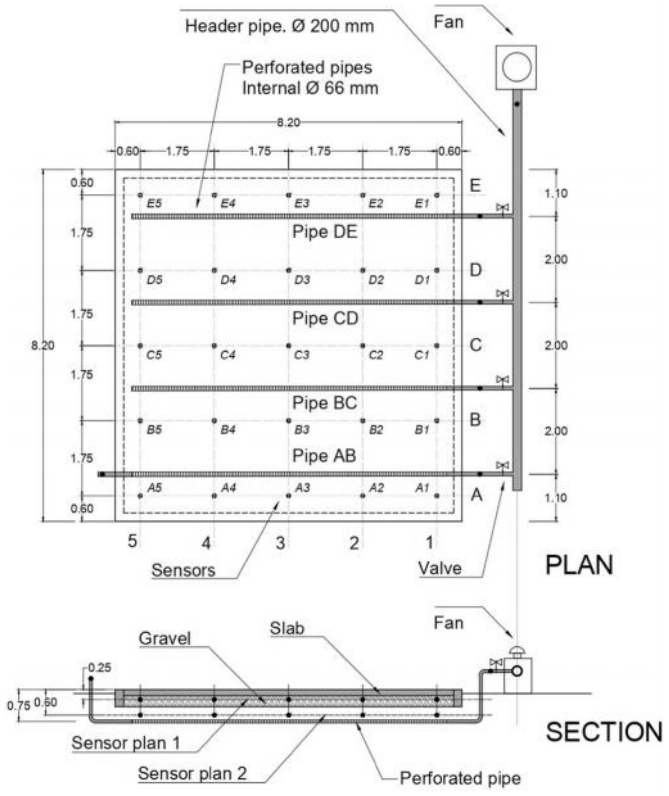

Fig. 2. Plan and section views of the slab with the measuring point grid, showing depressurisation system consisting of underground perforated pipes, an above-ground collector pipe and a mechanical extractor fan. (dimension in m).

- Perforated pipes: 75 mm outer and 66 mm inner diameter PVC elements, perforated with three groups of 5 cm long slots perpendicular to the length of the pipe, with the slots thus accounting for 22% of the total pipe wall area (Fig. 3).

The size of the slots and their impact on pressure drop at the area adjacent to the pipe wall was studied with COMSOL Multiphysics finite element simulation software. A mean pressure dropof 27% was observed between the inside and outside of the pipe.

- 200 mm diameter PVC header pipe with blank walls (Fig. 4).
- Cut-off valves on each perforated pipe for separate operation (Fig. 4).
- Soler y Palau Mixvent TH-800 120 W centrifugal extractor fan; maximum air flow, 775 m^3/h; maximum pressure, 450 Pa.

A photograph of the testing facility is reproduced in Fig. 4.

2.3. Multi-sensor pressure monitoring system

A number of perforated pipe setups were studied using Honeywell HSCDRRD006MDSA3 differential pressure sensors with an operating range of ±600 Pa and an accuracy of 3 Pa (Fig. 5b), positioned at predetermined points on a dual-depth grid underneath the slab. Other system components included a tmux terminal multiplexer, MSP modules to connect the sensors and a LabJack U3 data acquisition unit for connection to the computer. Developed by the CSIC's Physical and Information Technologies Institute (ITEFI-CSIC), the system, along with its components and sensitivity tests, is described in Sicilia et al. (2019). A module of the pressure sensor system is shown in Fig. 5b.

Readings were taken on two planes at different depths: plane 1, located at the interface between the bottom of the slab and the gravel fill, and plane 2, at 45 cm below the slab in the soil (Fig. 5a). Hollow steel tubes were driven into the soil to position plane 2, and perforated plastic spheres connected to 4 mm (inner ∅) soft polyurethane tubes were used to position the plane 1 sensors.

In addition to the 25 points per plane on the 5 × 5 grid (Figs. 5c and 2), a measuring point located outside the area covered by the slab was installed as a reference. The pressures in the fan and at the head of each pipe were also recorded.

The differential pressure readings at each point relative to the exterior were recorded simultaneously at all points with software developed using MATLAB environment. The readings were recorded both on a timeline for each sensor and on a graphics display representing slab geometry. For further information about the visualization software see Sicilia et al. (2019).

After installing the pressure monitoring system, long-term tests were conducted to detect possible inter-sensor deviations. A sample of the findings for 5 days with the depressurisation system disconnected is reproduced in Fig. 6. In this test eight sensors were positioned at different points on the slab, four in the gravel plane (A3, A5, B3, C3 in Fig. 2) and four in the soil plane (B1′, B2′, C1′, C3' in Fig. 2).

All the sensors were checked for performance and adjusted and calibrated where deviations were detected. Minor diurnal cycle fluctuations (±2 Pa) were observed. The difference in density between the outdoor air and the air in the soil pores due to temperature differences and the effect of thermal inertia in the soil translated into slight variations in sensor pressure readings.

The effects of atmospheric agents on the pressure between the soil and overlying space were documented in some studies (Frutos et al., 2011; Groves-Kirkby et al., 2015; Hintenlang, 1992; Yang et al., 2019; Zafrir et al., 2013). Wind action may induce momentary alterations (pressure or suction) at one end of the differential pressure device

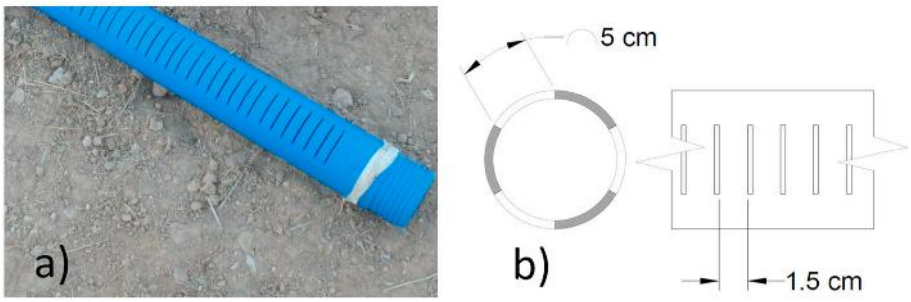

Fig. 3. a) Underground perforated pipe; b) cross-section and elevation view of the pipe used.

Fig. 4. Testing facility.

positioned on top of the slab. Here the pre-setup and system sensitivity studies revealed that rain could saturate the soil around the slab, raising the underlying pressure. In light of those considerations, all tests were conducted on similarly dry days, i.e., in the absence of rain for at least a full week. . The exposed part of the pressure device was sheltered in insulated casing to prevent superheating and direct wind action (Figs. 5c and 4).

3. Results and discussion

The behaviour of the pressure field induced underneath the slab was determined under different test setups. The findings described below were applied to analyse pressure field morphology and intensity on planes 1 and 2, the pressure induced by each pipe or combination and the impact of pipe spacing and fan power. In addition, the effect of combined operation was compared to the sum of the effects of the pipes involved.

The pressure monitoring system described in section 2.3 logged the data at one reading per second, with the system programmed to record the mean of every five readings.

The procedure deployed for the experiments was as follows: no readings were taken in the first 5 min after activating the depressurisation system to ensure pressure had stabilised (which normally takes no more than 1–2 min). Data were then recorded in the following 5 min and averaged to deliver the final reading. The tests were conducted in two phases, first for plane 1 and then for plane 2. Data consistency was ensured by duplicating a four-point pressure line (B4, C4, D4, E4) and simultaneously logging the readings on both planes in every experiment.

The results of each test are discussed and analysed below.

3.1. Pipe-by-pipe pressure field distribution in planes 1 (gravel) and 2 (soil)

Seven pipe operation setups were studied. In setup 0 the fan was off; in 1–3 each pipe was activated separately; and in 4 through 7 different combinations of pipes were activated jointly. No results for setups involving pipe AB are reported for the reasons set out in section 2.2.

The results are summarised in Fig. 7. Each matrix cell gives the findings (Pa) for the two planes: the upper value for plane 1, gravel, and

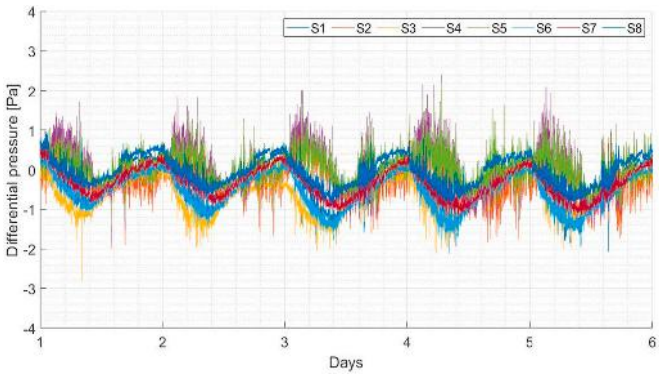

Fig. 6. Pressure readings over 5 days (21–26 August) with depressurisation system disconnected.

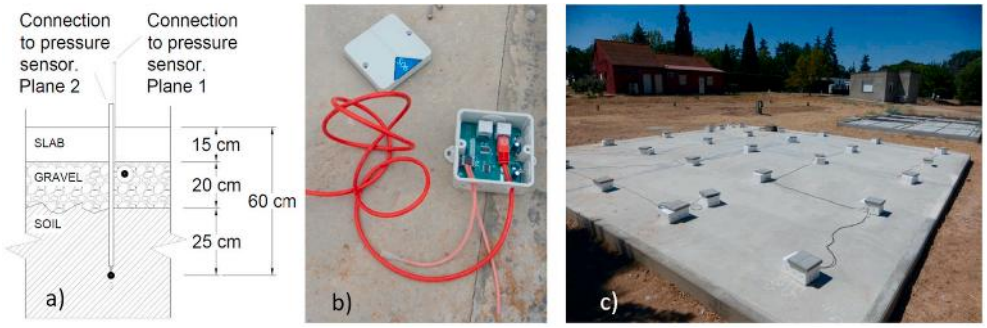

Fig. 5. a) Cross-section showing pressure sensor depths; b) pressure sensor; c) finished slab with sensors in place.

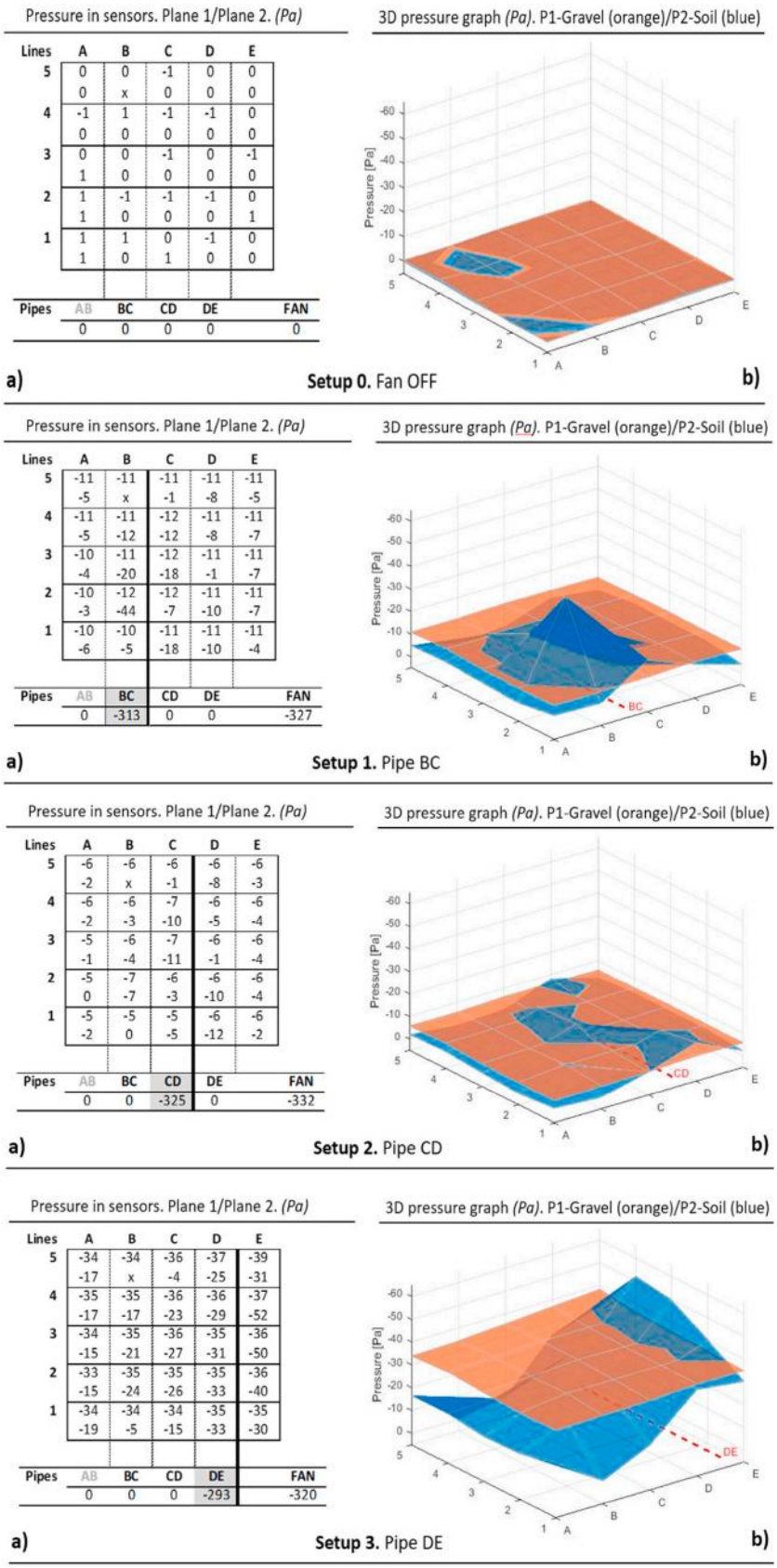

Lines	A	B	C	D	E
5	0	0	-1	0	0
	0	x	0	0	0
4	-1	1	-1	-1	0
	0	0	0	0	0
3	0	0	-1	0	-1
	1	0	0	0	0
2	1	-1	-1	-1	0
	1	0	0	0	1
1	1	1	0	-1	0
	1	0	1	0	0

Pipes	AB	BC	CD	DE	FAN
	0	0	0	0	0

Lines	A	B	C	D	E
5	-11	-11	-11	-11	-11
	-5	x	-1	-8	-5
4	-11	-11	-12	-11	-11
	-5	-12	-12	-8	-7
3	-10	-11	-12	-11	-11
	-4	-20	-18	-1	-7
2	-10	-12	-12	-11	-11
	-3	-44	-7	-10	-7
1	-10	-10	-11	-11	-11
	-6	-5	-18	-10	-4

Pipes	AB	BC	CD	DE	FAN
	0	-313	0	0	-327

Lines	A	B	C	D	E
5	-6	-6	-6	-6	-6
	-2	x	-1	-8	-3
4	-6	-6	-7	-6	-6
	-2	-3	-10	-5	-4
3	-5	-6	-7	-6	-6
	-1	-4	-11	-1	-4
2	-5	-7	-6	-6	-6
	0	-7	-3	-10	-4
1	-5	-5	-5	-6	-6
	-2	0	-5	-12	-2

Pipes	AB	BC	CD	DE	FAN
	0	0	-325	0	-332

Lines	A	B	C	D	E
5	-34	-34	-36	-37	-39
	-17	x	-4	-25	-31
4	-35	-35	-36	-36	-37
	-17	-17	-23	-29	-52
3	-34	-35	-36	-35	-36
	-15	-21	-27	-31	-50
2	-33	-35	-35	-35	-36
	-15	-24	-26	-33	-40
1	-34	-34	-34	-35	-35
	-19	-5	-15	-33	-30

Pipes	AB	BC	CD	DE	FAN
	0	0	0	-293	-320

Fig. 7. Pressure data in setups 0 to 7. a) pressure readings at all measuring points on both planes under different combinations of active pipes; b) 3D graphic of field morphology (orange - gravel; blue - soil). (For interpretation of the references to colour in this figure legend, the reader is referred to the Web version of this article.)